FINITE ELEMENT ANALYSIS OF PLATES WITH THROUGH CRACKS FROM HIGHER ORDER PLATE THEORY

S. Viswanath*, M. V. V. Murthy* and K. P. Rao**

*Structures Division. NAL. Bangalore. India
**Aerospace Department. IISc. Bangalore. India

ABSTRACT

A special crack tip element for plate bending is developed using general crack tip solutions derived from a continuum analysis through Reissner's theory. It is demonstrated that using this in combination with a conventional shear flexible element, accurate results for bending stress intensity factor can be obtained over a wide range of a plate thickness parameter.

KEY WORDS

Fracture, Stress Intensity Factor, Plate bending theory, Crack-Tip Finite Element.

INTRODUCTION

Earlier analytical works (Knowles and Wang, 1960; Hartranft and Sih, 1968; Wang, 1968)on the bending of plates with cracks, taking shear deformation into account, have shown that the classical theory prediction (Williams, 1961) of stresses in the vicinity of the crack is erroneous with respect to the angular distribution of stresses. Consequently, the prediction of bending Stress Intensity Factor(SIF), which is dependent on plate thickness, from classical plate theory would not be meaningful. Hartranft and Sih(1968) showed that the SIF for an infinite plate varies very rapidly in the h/a range of 0 to 0.25, where h is the plate thickness and a is the semi-crack length. Further, the SIF Vs h/a curve is shown to have an infinite slope at h/a = 0. It is seen from their results that even for h/a as small as 0.2, the SIF is 62 percent greater than that given by Knowles and Wang (1960) for h/a ---> 0.

Thus, there is a need for a closer examination of the variation of SIF with the thickness of plate through a higher order plate theory.

Various types of finite element formulations have been attempted accounting for the singularity near the crack tip in a plate under bending. A few of the special crack elements available have the defect that they are based on classical plate theory (Wilson and Thomson, 1971; Ahmad and Loo, 1979) which is erroneous. A quarter point singular element proposed by Barsoum (1976) based on shear deformation theory appears to be more accurate for thicker plates ($h/a\sqrt{10}>0.5$) than for thin plates. Yagawa and Nishioka (1979) have presented a superposition method together with reduced integration technique for an element based on shear deformation theory, but the crack-tip displacement field (W) description used in the analytical part of the solution for the element was still based on the classical plate bending theory. Recently, Rhee and Atluri (1982) have presented the bending analysis of a plate with a crack by a hybrid stress model based on Reissner's theory. The regular elements used in the plate modelling are based on Kirchhoff assumption. This led to some difficulties in interpreting the rotational degrees of freedom at the interface while .assembling with the crack tip element based on shear deformation. Moriya (1979) developed an assumed stress hybrid model in the form of superelements based on Reissner's theory.

In the present work, the development of a special crack-tip element for mode I type of bending based on a general solution (Murthy, Raju and Viswanath, 1981) is presented. A special feature of the element development is that the stiffness matrix is obtained by integration over the element boundary rather than by the usual area integration thus resulting in improved accuracy and saving in computational effort. The effect of plate thickness on the bending stress intensity factor is studied over a wide range of h/a covering very thick to very thin plates.

Development of Special Crack-tip Element

Development of the special crack-tip element here is based on minimisation of total potential energy. The displacement field chosen satisfies the governing equations exactly and is taken from (Murthy, Raju and Viswanath, 1981). The displacement field in dimensional form is given by

$$W_\mu = r^{\mu+2}\left[A_\mu \cos\mu\theta + B_\mu \cos(\mu+2)\theta\right] \qquad (1)$$

$$\chi_\mu = \sum_{n=0,1,2,\cdots}^{\infty} C_{\mu+2n}\ \bar{\chi}_{\mu+2n} \qquad (2)$$

$$\bar{\chi}_\mu = \sin\mu\theta \sum_{m=0,1,2,\cdots}^{\infty} \frac{k^{2m} r^{\mu+m}}{\lfloor m\ \phi(\mu,m)} \qquad (3)$$

$$\phi(\mu, m) = (\mu+1)(\mu+2)\cdots(\mu+m) \quad \text{for } m \geqslant 1$$

$$= 1 \text{ for } m=0$$

where (r,θ) are the polar coordinates (Fig.1), W is the normal displacement, χ is a stress function in Reissner's theory, is an eigen value in the solution taking fractional as well as integer values - 1 1/2, 3/2, 5/2,....∞ and 0, 1, 2, 3.. ..,∞,

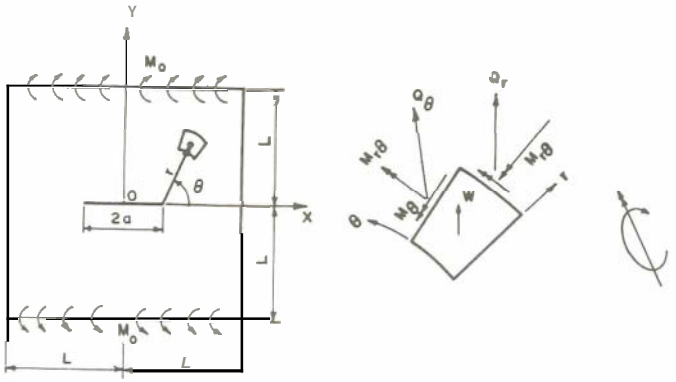

Fig.1 System of coordinates and stress resultants

The constants in equations (1) and (2) are connected through the relations:

$$C_{(\mu+2n),F} = \frac{4D(\mu+1)(-k^2)^n}{\lfloor n \ \phi(\mu+n-1,n)} A_{\mu,F} \qquad (4)$$

$$B_{\mu,F} = -\frac{[4+(1-\nu)\mu]}{(1-\nu)(\mu+2)} A_{\mu,F} \qquad (5)$$

$$C_{\mu+2n,I(1)} = \frac{4D(-k^2)^n}{\lfloor n-1 \ \phi(\mu+n,n)} \left[\frac{\mu(\mu+1)}{n(\mu+n)} + 2 - \frac{(\mu+2)(1-\nu)}{2}\right] A_{\mu,I(1)}$$

$$- \frac{2(\mu+2)(1-\nu)(-k^2)^n}{\lfloor n-1 \ \phi(\mu+n,n)} B_{\mu,I(1)} \quad \text{for } n \neq 0, \ \mu \neq 0,1 \qquad (6)$$

$$= \frac{4D(-k^2)^n}{\lfloor n-1 \ \phi(\mu+n,n)} \left[2 - \frac{(\mu+2)(1-\nu)}{2}\right] A_{\mu,I(1)}$$

$$- \frac{2(\mu+2)(1-\nu)(-k^2)^n}{\lfloor n-1 \ \phi(\mu+n,n)} B_{\mu,I(1)} \quad \text{for } n \neq 0, \ \mu = 0,1 \qquad (7)$$

$$= 4(\mu+1)\, D\, A_{\mu, I(1)} \quad \text{for } n=0,\ \mu \neq 0, 1 \tag{8}$$

$$= 0 \quad \text{for } n=0,\ \mu = 0, 1 \tag{9}$$

$$W_{I(2)} = 0, \quad \chi_{I(2)} = \sum_{n=0,1,2,\cdots}^{\infty} C_{1+2n, I(2)}\ \bar{\chi}_{1+2n} \tag{10}$$

$$C_{1+2n, I(2)} = \frac{D(-k^2)^n}{\lfloor 2n+1} C_{1, I(2)}, \quad \text{where } k^2 = \frac{5}{2h^2} \tag{11}$$

$$W_R = A_R + B_R\ r\cos\theta \ ; \quad \chi_R = 0 \tag{12}$$

In the equations (4) to (12), the various subscripts correspond to different types of solution as below:

F : Solution for fractional μ
I(1) : First type of solution for integer μ
I(2) : Second type of solution for integer μ
R : Rigid body mode.

Singular stresses arise from $\mu = -1/2$ and are given by

$$\sigma_r = \left(\frac{6D}{h^2}\right) \frac{A_{-1/2}(1+\nu)}{\sqrt{r}} \left[\frac{5}{4}\cos\frac{\theta}{2} - \frac{1}{4}\cos\frac{3\theta}{2} \right] + O(1) \tag{13}$$

$$\sigma_\theta = \left(\frac{6D}{h^2}\right) \frac{A_{-1/2}(1+\nu)}{\sqrt{r}} \left[\frac{3}{4}\cos\frac{\theta}{2} + \frac{1}{4}\cos\frac{3\theta}{2} \right] + O(1) \tag{14}$$

$$\tau_{r\theta} = \left(\frac{6D}{h^2}\right) \frac{A_{-1/2}(1+\nu)}{\sqrt{r}} \left[\frac{1}{4}\sin\frac{\theta}{2} + \frac{1}{4}\sin\frac{3\theta}{2} \right] + O(1) \tag{15}$$

where $D = E h^3/12(1-\nu^2)$ and ν is Poisson's ratio.

Following the usual definition, the bending stress intensity factor $\bar{K}_I$ in the non-dimensional form is defined as

$$\bar{K}_I = \frac{\sqrt{2}\, D\, A_{-1/2}(1+\nu)}{M_0 \sqrt{r}} \tag{16}$$

where the nondimensionalization is done with respect to $\sigma_0 a$, σ_0 being a reference stress due to a reference bending moment M_0, $\sigma_0 = 6 M_0/h^2$.

Minimization of total potential energy of the crack-tip element is now carried out converting the area integral into boundary integrals through Green's theorm in the usual way. As the displacement field chosen satisfies the governing equations exactly, the resulting area integral vanishes identically. The minimization procedure thus leads to

$$\delta\pi = \int_{\Gamma} [(M_n - \bar{M}_n)\delta\beta_n + (M_{nt} - \bar{M}_{nt})\delta\beta_t + (Q_n - \bar{Q}_n)\delta W]\, ds = 0 \qquad (17)$$

where M, Q, β denote moments, transverse shear forces and rotations, Γ denotes boundary of the element, s denotes length coordinate measured along the boundary, (n,t) denote directions normal and tangential to Γ, and $\bar{M}_n$, $\bar{M}_{nt}$, $\bar{Q}_n$ denote applied traction forces on the boundary.

In the above equation, δ stands for variation. The variation is carried out with respect to each 'independent constant' in the solution given by equation (1). Here 'independent constant' is one which remains independent in view of the relations (4)-(9) and (11). It is to be noted that for fractional μ, only A is independent whereas for integer μ, A and B are both independent.

Let us for instance consider variation with respect to an independent constant $A_{1/2}$. Here $\delta\beta_n$ is to be interpreted as $\beta_{n,1/2}\,\delta A_{1/2}$ where $\delta\beta_{n,1/2}$ correponds to β_n for unit value of $A_{1/2}$. Equation (17) is written for each independent constant and a congruent transformation is carried out connecting the constants and the physical degrees of freedom at the nodes which are chosen as W, β_x and β_y. This leads to the stiffness matrix as well as consistent load vector for the special crack tip element.

From the foregoing formulation, it is seen that any shape can be chosen for the crack tip element by using numerical integration over the boundary in equation (17). However, the choice is governed from consideration of interfacing the crack tip element with conventional elements. A survey of the literature revealed that perhaps the best conventional shear flexible element is a simple 4-noded quadrilateral element (Prathap and Viswanath, 1983). This element avoids the usual 'shear locking' and behaves well in a wide range of plate thickness. This is achieved by an optimal integration scheme for the shear energy of the element. However, a limitation arises from the direction dependence of the coordinate for the integration scheme. The best results are obtained if the element is rectangular in shape. From this consideration, the crack tip element was also chosen to be rectangular.

Earlier continuum analysis of rectangular plates with cracks by the authors revealed that best results are obtained if the aspect ratio of plates is 2 : 1. This was found to lead to minimum boundary errors because all parts of the boundary would be equidistant from the crack tip.

The number of nodal points required for the crack tip element to give satisfactory results should depend on the element size. There is an optimum value for the element size itself an aspect which is discussed at length in the next section. For this optimum size the number of nodal points required is found to be thirteen as in Fig. 2. As $\beta_y = 0$ at the nodal point on the plane of symmetry, the total number of degrees of freedom should be 38. However, the SIF-K_I is also introduced as a degree of freedom so that the total number of degrees of freedom for the crack tip element is 39.

Integration in equation (17) is carried out by using Gaussian quadrature. Each side of the element is divided into an appropriate number of segments depending on the number of harmonics occuring in the solution ensuring that not more than one extremum occurs over each segment. With this, it was found sufficient to use 5 point Gaussian quadrature integration over each segment. In evaluating the integral numerically, the crack boundary and the symmetric lines were excluded as the integral vanishes here identically in view of the boundary conditions for the crack boundary and symmetric conditions for the line of symmetry.

Results and Discussion

In order to assess the efficiency of the special crack tip element developed, the problem of a square plate with a central crack under uniform edge bending, shown in Fig.1, was considered. In view of double symmetry, only a quardrant of the plate as shown in Fig. 2 was discretized.

From the numerical study, it was found that the SIF obtained was dependent upon the size of the crack tip element. Similar observation was also made by Rhee and Atluri(1982). Fig.3 shows a plot of SIF Vs h/c for L/a=2 and for various values of h/a. It is seen that the degree of sensitivity of the results increases with decrease in h/a. It is also seen that the SIF reaches a peak at $h/c \simeq 1$ for all h/a. The existence of such an optimum value for h/c can be explained. If the crack tip element is too large, the errors on the element boundary become large because the Bessel functions in the solution grow expoentially away from the crack tip. If the crack tip element is too small, three dimensional effects dominate and the element can no longer be modelled as a plate. All subsequent computations are carried out with crack tip element size corresponding to h/c=1.

Computations were carried out for a square plate with a central crack for L/a=10. This value of L/a was chosen so as to correspond approximately to an infinite plate for which continuum solutions are available (Hartranft and Sih, 1968). Fig. 4 shows a plot of the nondimensional SIF against h/a. It may be seen that correlation with the continuum solution results of Hartranft and Sih (1968) is good. For small h/a (h/a < 0.25), the SIF varies very rapidly with h/a and Hartranft and Sih (1968) showed that at h/a=0 the slope of the curve in Fig. 4 is infinity. Thus, the results for h/a < 0.5 are plotted to a different scale in Fig. 5 covering h/a ratios as low as 0.02.

A distinguishing feature of the present investigation is that very low values of h/a are covered compared to earlier finite element investigations. For instance, the lowest value of h/a covered in (Yagawa and Nishioka, 1979 ; Rhee and Atluri, 1982 ; Moriya, 1979) are 0.1, 0.1 and 0.2 respectively. Apparently, it is possible that convergence difficulties were encountered for lower h/a in these studies. As the continuum solution curve has infinite slope at h/a=0, there were difficulties in scaling off the results and hence comparision with the results of (Hartranft and Sih, 1968) is not shown in Fig.5 for h/a < 0.1. However, it may be seen that the theoretical limit of $K = (1+\nu)/(3+\nu) = 0.3939$ is being approached with infinite slope at h/a=0 by the results of present analysis.

Concluding Remarks

It appears that the present investigation to be the first of its kind where the stress and displacement description in the crack tip element for the bending case is fully based on a continuum solution. It is found that there exists an optimum size for the crack tip element. Further, the shape of this element and its size in relation to the thickness has been established. With the special element developed, it is found possible to cover very low h/a ratio not covered in the earlier crack tip element formulations.

REFERENCES

Ahmad, J., and F.T.C. Loo (1979) Engng Fract. Mech 11, 661-673.

Barsoum, R.S (1976) Int.J.num. Meth. Engng. 10, 551-564.

Hartranft, R.J., and G.C. Sih (1968) J.Math and Phy., 47, 276-291.

Knowles, J.K., and N.M. Wang (1960) J.Math and Phy., 39, 223-236.

Moriya, K (1979) Proc. Japan Natl. Cong. Theor. & Appl. Mech., 29.

Murthy, M.V.V., K.N. Raju and S. Viswanath (1981) Int.J.Fract. Mech., vol. 17, No. 6, 537-552.

Prathap, G., and S. Viswanath (1983) IJNME., 19, 831-840.

Rhee, H.C., and S.N. Atluri (1982), IJNME., 18, 259-271.

Wang, N.M., (1968) J.Math and Phy., 47, 371-390.

Williams, M.L (1961) Journal of Applied Mechanics, 28, 78-82.

Wilson, W.K., and D.G. Thomson (1971) Engng. Fract. Mech 3, 97-102.

Yagawa, G., and T. Nishioka (1979), IJNME., 14, 727-740.

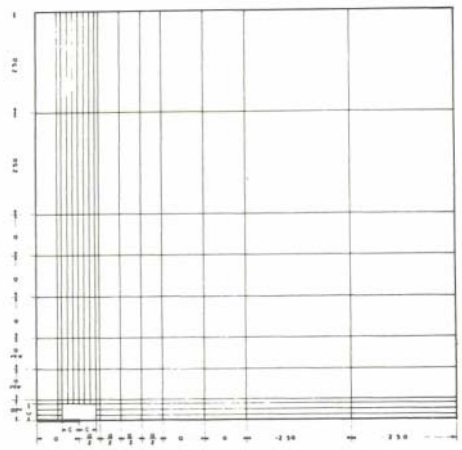

Fig.2. Mesh representation of a quarter plate

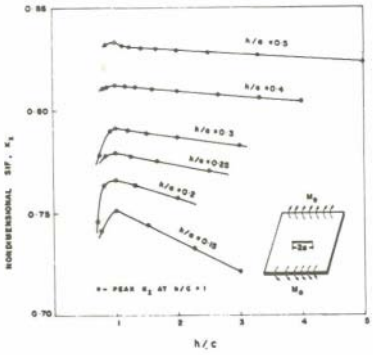

Fig.3. Variation of SIP with h/c ratio

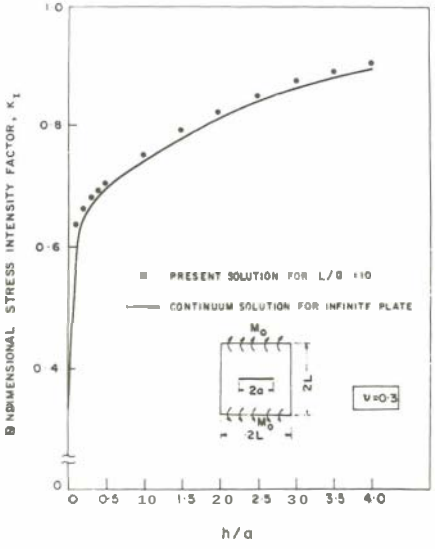

Fig.4. SIF Vs h/a Ratio

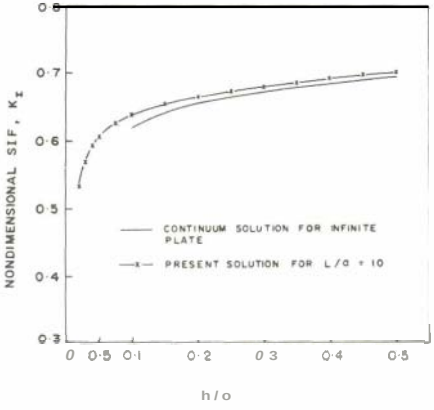

Fig.5. SIF Vs h/a Ratio